Agricultural Research & Technology
Open Access Journal
ISSN: 2471-6774

Juniper Publishers
key to the Researchers

Research Article
Volume 28 Issue 5 - September 2024
DOI: 10.19080/ARTOAJ.2024.28.556425

Agri Res & Tech: Open Access J

Spatial Analysis of UAS-generated Data to Evaluate Nitrogen Fertilizer Placement Alternatives, Predict and Map End-of-Season Rice Yield

Andrew Manu[1]*, Vincent Kodjo A[2], Thomas JL[3], Ama Twumasi D[1], and Amisu Mohammed[2]

[1]*Iowa State University, USA*

[2]*University for Development Studies*

[3]*Indigo Ag*

Submission: September 03, 2024; **Published:** September 13, 2024

***Corresponding author:** Andrew Manu, Lowa State University, USA

Abstract

Urea deep placement (UDP), which directly targets nitrogen (N) to the root zone, has shown promise in enhancing crop uptake, yield, and environmental sustainability compared to other N placement methods (non-UDP). This study utilized unmanned aerial systems (UAS or drones) to evaluate the impact of different N placement strategies on rice spectral signatures across three production zones, with an average farmer field size of 11.4 hectares. The research focused on analyzing Normalized Difference Vegetation Index (NDVI) and Optimized Soil Adjusted Vegetation Index (OSAVI) reflectance from UAS flight data collected during the booting stage in three rice health zones defined as low $_{(NDVI\ 0.728)}$, medium $_{(NDVI\ 0.874)}$, and high $_{(NDVI\ 0.914)}$. End-of-season rice grain yields revealed a nonlinear relationship with NDVI on the plot scale, whereas OSAVI exhibited a significant linear correlation with plot yields across the different zones. Spatial analysis, supported by the Jenks natural breaks algorithm, categorized OSAVI reflectance into four homogeneous groups, enabling predictions of rice yields at the plot scale and extrapolating plot yields to farmer field levels. This approach refined assessment outcomes, effectively distinguishing between UDP and non-UDP treatments. The UDP N management consistently outperformed other N placement methods, with yield increases of 9.9% at the plot level and 14.3% at the farmer field level. Additionally, this spatial analysis facilitated the generation of high-resolution digital yield maps, providing a valuable tool for precision agriculture to optimize N management and enhance overall productivity in rice cultivation.

Keywords: Unmanned Aerial Systems (UAS); urea deep placement (UDP); crop health; NDVI; OSAVI; Jenks Natural Breaks Algorithm; Upscaling

Abbreviations: UDP: Urea Deep Placement; N: Nitrogen; NDVI: Normalized Difference Vegetation Index; OSAV: Optimized Soil Adjusted Vegetation Index; USAID: United States Agency for International Development; IFDC: International Fertilizer Development Center; USG: Urea Super Granules; SPOT: Satellite Pour l'Observation de la Terre; TIS: Tono Irrigation Scheme; GPS: Global Positioning System; SODA: Sensor Optimized for Drone Applications; Ca: Calcium; Mg: Magnesium; K: Potassium; Na: Sodium; ECEC: Effective Cation Exchange Capacity; ANOVA: Analysis of Variance; OM: Organic Matter; CEC: Cation Exchange Capacity; TN: Total Nitrogen; CVs: Coefficients of Variation; UAS: Unmanned Aerial System

Introduction

Rice (Oryza sativa L.) is Ghana's second most crucial staple grain and a profitable cash crop for local farmers [1,2]. Ghana's annual per capita rice consumption has risen significantly from 17.5 kg during 1999-2001 to 24 kg in 2010-2011, with projections indicating an increase to 51.63 kilograms by 2020 [3,4]. Despite this growth, Ghana relies on imports for 66% of its rice consumption. Low yields play a significant role in this imbalance, with a national average of 3.28 mt ha^{-1} compared to an attainable yield of 6.0 mt ha^{-1} [5]. Rice productivity in Ghana faces a significant challenge due to low soil fertility, typically linked to reduced organic carbon levels, as well as limited availability of nitrogen (N) and phosphorus (P) [6,7]. Other social constraints further contribute to the widening gap between local production and imports. Notable issues include the high cost of improved seeds, limited access to credit, and inadequate processing facilities [8].

Despite a marginal increase in rice production to around 651,000 tons of milled rice in 2020 [9], an estimated $450 million is allocated annually for rice imports to meet local demand [10]. The Government of Ghana has recently intensified efforts to

develop the local rice sector, collaborating with international organizations like the United States Agency for International Development (USAID). This collaborative initiative aims to bolster national rice security, generate youth employment opportunities, stimulate economic growth, and alleviate poverty. Research by [11] suggests that implementing appropriate policy measures could narrow the gap between domestic rice production and imports. Nitrogen emerges as a crucial yet limiting factor within rice production systems. Be-yond maximizing rice yield, N is pivotal in ensuring grain yield quality [12]. The substantial N requirement underscores the need for efficient management to enhance productivity. Traditionally, farmers employ surface broadcasting of N-containing fertilizers for N application. However, N use efficiency (NUE) is notably low, ranging between 30% and 50% [13]. Factors contributing to N loss include high levels of ammonia volatilization up to 50% of applied N, denitrification, leaching, and surface runoff [14,15].

The urea deep placement technology development emerged from a collaboration between the International Fertilizer Development Center (IFDC) and primarily Bangladeshi farmers [16]. A comprehensive examination of the technology's features and impact is outlined in the works of [17,18]. This farmer-friendly advancement enhances NUE in rice production by mitigating N loss through volatilization [19,20], thereby boosting rice productivity. Urea super granules (USG) briquettes, acting as N carriers in this technology, exhibited a 25 percent increase in rice grain yield when applied at a rate of 56 kg N ha^{-1} compared to the recommended dose of 100 kg N ha^{-1} using the conventional urea broadcast method in Indonesia [21]. Similar positive outcomes were observed in Ghana, Nigeria, and Burkina Faso [22-24].

Accurate and timely assessments of rice field extents and their potential production capacity are essential for governmental bodies, planners, and decision-makers [25]. However, existing national statistics on crop production capacities often rely on field surveys and farmer interviews. Besides occasional inaccuracies, these data acquisition methods can be exceptionally time-consuming, labor-intensive, and cost-ineffective. Additionally, there is often a notable delay between data collection, collation, and reporting [26].

Remote sensing has been employed for monitoring and mapping extensive fields through satellite imagery. [27] combined optical and radar satellite data from the Satellite Pour l'Observation de la Terre (SPOT) to improve the accuracy of rice yield predictions in Taiwan. Similarly, [28] suggested a multi-satellite approach to assess the growth status of rice plants and determine the protein content of rice grains. Additionally, [29] used multispectral imagery from Landsat ETM+ to produce NDVI data, which was subsequently used to evaluate rice crops' health and growth stages.

Vegetation indices are crucial in remote sensing, assessing vegetation's presence and condition. Additionally, VIs can gauge variations in physiological state and biophysical properties [30], monitor crop growth, and evaluate vegetation stress and crop yields [31,32]. VIs rely on the photosynthetic responses of green vegetation to incident light. A high VI, termed "high health" in this context, results from high reflectance in the infrared region of the electromagnetic spectrum and low reflectance due to chlorophyll absorption in the red spectrum. Conversely, stressed, unhealthy, or deceased vegetation exhibits a low VI, referred to as "low health," attributed to diminished chlorophyll pigment [33]. Challenges in remote sensing include low spectral and temporal resolution and cloud cover [34]. Furthermore, [35] suggested that this technology is beneficial mainly for extensive studies and may not be suitable for the smaller-scale farming systems commonly found in Africa and Asia.

Over the past decade, UAS applications have expanded significantly. Unmanned platforms provide greater

versatility and flexibility over satellites or other airborne systems. UAVs can operate at low altitudes, capturing images with high temporal and spatial resolution [36-38]. These characteristics enable UAS remote sensing to address research inquiries and apply the technology in practical field scenarios. NDVI is computed based on light intensities reflected from canopies in the visual and near-infrared range [39]. This index holds immense potential for extracting information about dynamic changes in various vegetation types, making it a valuable tool for investigating spatial and temporal variations in diverse plant cover [40]. However, it has been observed that NDVI reaches saturation levels when estimating biomass in fully developed canopies [41,42]. However, several other VIs have been created to examine spatial and temporal variations and remain sensitive when NDVI saturates with OSAVI) [43] being one such index. In addition, OSAVI incorporates a soil adjustment coefficient (0.16) to mitigate variations in soil background conditions.

This study aims to achieve two interrelated objectives, each supported by a pair of hypotheses. For the first objective, hypothesis H1a posits that different N placement methods affect end-of-season rice production. Hypothesis H1b suggests that spectral signatures from UAS data can reliably predict the effects of these N placement methods. For the second objective, hypothesis H2a asserts that vegetation indices, such as OSAVI, strongly correlate with rice yields, allowing for accurate prediction of field-scale rice production. Hypothesis H2b proposes that visualizing the OSAVI-yield relationship across the landscape can identify high and low-productivity areas, providing valuable insights for agricultural intervention.

The objectives of this study are to:

a) Investigate the use of UAS technology-acquired data to compare the impact of different N placement alternatives on crop spectral signatures and resulting end-of-season rice production.

b) Predict field-scale rice yields using OSAVI and visualize how the OSAVI-yield relationship manifests across the landscape.

How to cite this article: Andrew M, Vincent Kodjo A, Thomas J, Ama Twumasi D, Amisu M. Spatial Analysis of UAS-generated Data to Evaluate Nitrogen Fertilizer Placement Alternatives, Predict and Map End-of-Season Rice Yield. Agri Res& Tech: Open Access J. 2024; 28(5): 556425. DOI: 10.19080/ARTOAJ.2024.28.556425

Materials and Methods

Site Characterization

The research was conducted within the Tono Irrigation Scheme (TIS) (latitude 10° 52'N; longitude -1° 11'W) situated in the Kassena-Nankana East District of the Upper East Region of Ghana (Figure 1a). This gravity-fed irrigation system operates on reservoir storage, boasting a total capacity of 93 million m^3 and covering a catchment area of 650 km^2 (Figure 1b). The scheme is designed to irrigate 3,840 hectares of land potentially, yet it currently provides irrigation to 2,490 hectares, predominantly dedicated to rice cultivation. This scheme comprises 4,000 smallholder producers and the average farmer field sizes range from 0.2 to 0.6 hectares.

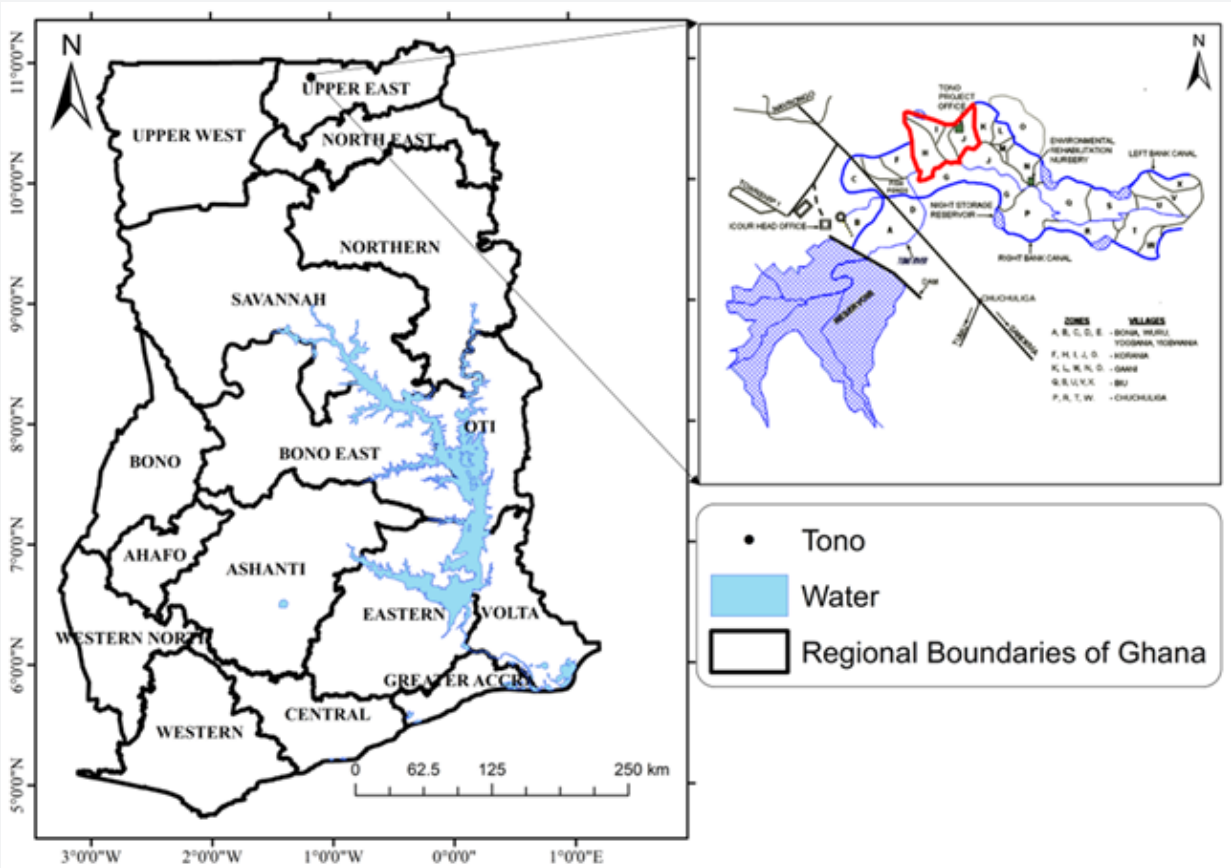

Figure 1: (a) Map showing the location of the Tono Irrigation Scheme in the Upper East Region of Ghana: (b) Schematic of the reservoir serving perimeter and the rice production areas showing zones H, I, and J.

Farmer Volunteers and Field Ground Mapping of Producer Fields

Farmers from zones H, I, and J (Figure 1b) volunteered for the study based on their N management preferences. The initial group, UDP farmers, showed a keen interest in experimenting with the emerging UDP N management technology. The second group consisted of non-UDP volunteers, an independent set of farmers with plots within the three zones who had not yet adopted the UDP technology. These farmers autonomously performed various agricultural tasks, including land preparation, seedling raising in nurseries, transplanting, fertilizer application, weed and pest control, and field harvesting. Fifty volunteers participated in this study, with 25 assigned to each UDP and non-UDP N management group. The distribution of farmers across the three zones is outlined in (Table 1).

Field sizes varied between 0.15 and 2.7 hectares, with an average of 0.62 hectares. Zone J had the largest average field size among the three zones, measuring 0.86 hectares. This contrasted significantly with Zone H (0.52 hectares) and Zone I (0.4 hectares).

How to cite this article: Andrew M, Vincent Kodjo A, Thomas J, Ama Twumasi D, Amisu M. Spatial Analysis of UAS-generated Data to Evaluate Nitrogen Fertilizer Placement Alternatives, Predict and Map End-of-Season Rice Yield. Agri Res& Tech: Open Access J. 2024; 28(5): 556425. DOI: 10.19080/ARTOAJ.2024.28.556425

Table 1: Volunteer Farmers and their farm sizes within zones H, I, and J.

Zone	Non-UDP		UDP	
	Number of volunteers	Total farm size (ha)	Number of volunteers	Total farm size (ha)
H	4	1.5	9	3.2
I	5	3.2	4	1.6
J	16	15.7	12	8.9

UAS Remote Sensing and Image Processing

At the beginning of the study, we used a handheld Garmin SD MAP 64sc global positioning system (GPS) unit to delineate the boundaries of each farmer's rice field. Subsequently, we utilized ArcGIS Pro to estimate the sizes of farmers' fields based on the coordinates of their field boundaries. It is crucial to highlight that the farmer field within each zone served as the basic unit for investigation and subsequent data analysis.

At the booting stage of the rice crop, low-altitude aerial surveys were conducted for zones H, I, and J (Figure 1b) as distinct units. The flight boundaries were established using field coordinates obtained from the initial ground GPS mapping. These coordinates were imported into eMotion, a SenseFly software [44], to generate autonomous flight plans for an eBee ag (Figure 2), a cost-effective agricultural drone. The eBee offers fully autonomous flight capabilities, from takeoff to landing, and is controlled via a user-friendly ground control software that allows for mission planning and real-time monitoring. This drone offers an extended flight time of up to 55 minutes and 160 hectares / 395 acres coverage. Two multispectral sensors were used, the Sequoia and the Sensor Optimized for Drone Applications (SODA). The Sequoia sensor captured images in the following four distinct bands: green $_{(530\text{-}5570\ nm)}$, red $_{(640\text{-}680\ nm)}$, near-infrared $_{(800\text{-}880\ nm)}$, and red edge $_{(710\text{-}740\ nm)}$. It also has an embedded 16 MP red $_{(640\text{-}680)}$, green $_{(530\text{-}5570\ nm)}$ blue $_{(450\text{-}500)}$ camera. The SODA camera captured the red $_{(640\text{-}680)}$, green $_{(530\text{-}5570\ nm)}$, and blue $_{(450\text{-}500)}$ bands.

Figure 2: Picture of eBee ag Drone (Sensefly (™).

How to cite this article: Andrew M, Vincent Kodjo A, Thomas J, Ama Twumasi D, Amisu M. Spatial Analysis of UAS-generated Data to Evaluate Nitrogen Fertilizer Placement Alternatives, Predict and Map End-of-Season Rice Yield. Agri Res& Tech: Open Access J. 2024; 28(5): 556425. DOI: 10.19080/ARTOAJ.2024.28.556425

The eBee Ag drone, coupled with the Sequoia camera, was flown at 127.4 meters above elevation data (AED), with a 60% fore lap and 80% lateral overlap, resulting in a 12.0 cm/pixel ground resolution. The same eBee was flown with the SODA camera at 74.3 meters with 65% forelap and 70% side-lap to achieve a 7.0 cm/pixel. The initial image processing phase involved the eMotion 3 software [44]. This software facilitated georeferencing, alignment, and stitching of images by identifying tie points in overlapping images. Subsequently, the processed data were transferred to Pix4D, where the Standard Ag multispectral processing option was employed to generate seamless high-resolution orthomosaics for Zones H, I, and J, as depicted in (Figure 3). Two vegetation indices, NDVI and OSAVI, were computed, and their respective formulas and references are provided in (Table 2). Reflectance imagery was produced for the two vegetation indices.

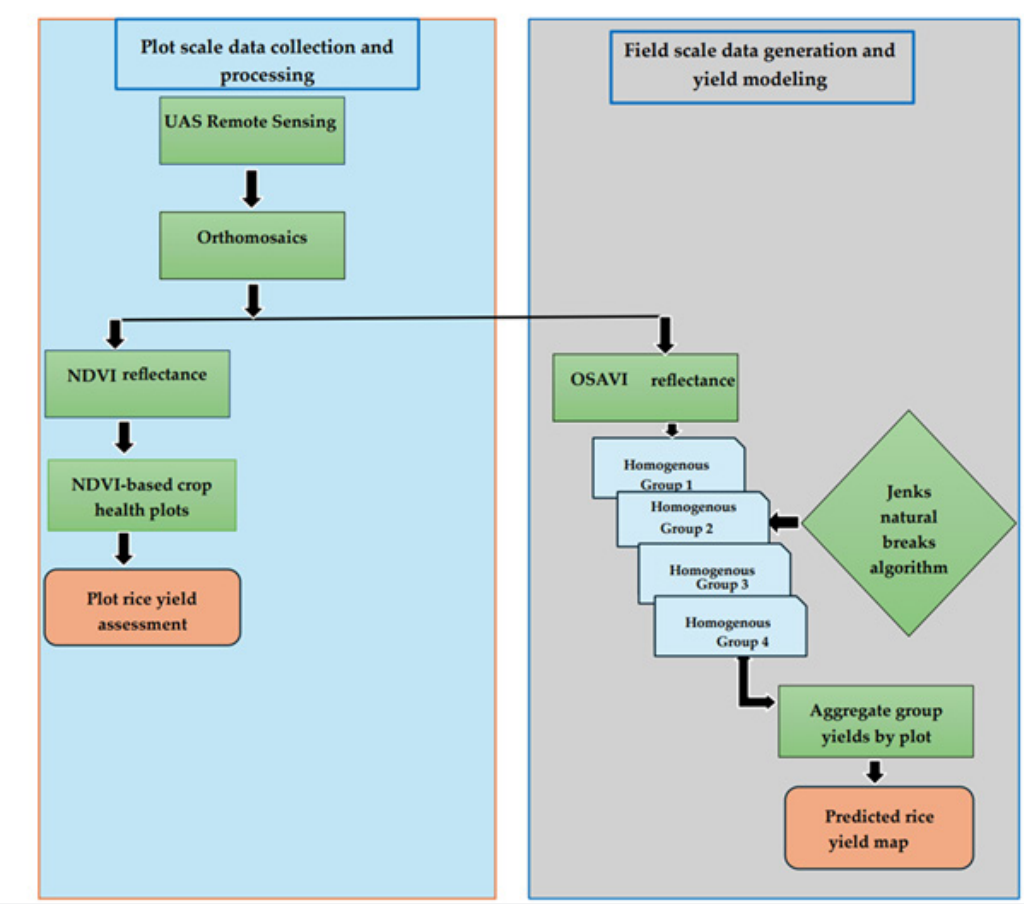

Figure 3: Overall research data collection and data analysis workflow.

Table 2: Summary of aerial sensors, spectral bands, and formulae used to measure the NDVI and OSAVI.

Vegetation Index	Sensor Type	Spectral Band	Central Wavelength	Formula	Reference
Normal difference vege-tation index (NDVI)	Sequoia Sensor Optimized for Drone Applica-tions (SODA)	Infrared	780	$NDVI = \frac{\rho NIR - \rho red}{\rho NIR + \rho red}$	[39]
		Red	670		
Vegetation Index (OSAVI)	Sensor Optimized for Drone Applications (SODA)	Infrared	780	$OSAVI = \frac{\rho NIR - \rho red}{\rho NIR + \rho red + 0.16}$	[40]
		Red	670		

How to cite this article: Andrew M, Vincent Kodjo A, Thomas J, Ama Twumasi D, Amisu M. Spatial Analysis of UAS-generated Data to Evaluate Nitrogen Fertilizer Placement Alternatives, Predict and Map End-of-Season Rice Yield. Agri Res& Tech: Open Access J. 2024; 28(5): 556425. DOI: 10.19080/ARTOAJ.2024.28.556425

Assessment of Crop Health Areas and Rice Grain Yield Determination

Three crop health plots were identified, designated as low, medium, and high, in farmers' fields based on NDVI values obtained from reflectance information and verified with visual assessment within the three zones. The NDVI values used to define crop health categories in UDP and non-UDP plots are presented in (Table 3). A total of 141 evenly distributed plots were identified, with 47 plots in each health zone category. These distinct areas of varying crop health contained contiguous pixels sufficient to establish $4m^2$ area plots. The coordinates of the four corners defining each health plot were recorded, and these $4m^2$ zones subsequently served as sampling plots for yield assessment. The average NDVI and OSAVI values for each $4m^2$ plot were also recorded from the reflectance map.

Table 3: Selected physical and chemical properties of the surface soil (0 -25 cm) by zones, N management system, and their intercorrelations.

Zone	Sand	Silt	Clay	pH	P	OM	T N	CEC
	%	%	%	%	%	%	%	cmol(+) kg-1
H	54.7b†	27a	18.76a	5.4a	5.08b	1.94a	0.11a	18.38a
I	70.6a	16.7b	13.1b	5.7a	2.32c	1.16b	0.07b	7.48b
J	56.7b	28.7a	14.6b	5.9a	6.58a	1.23b	0.10b	7.94b
Soils under UDP and non-UDP management								
Non-UDP	55.1a	27.7a	17.3a	5.6a	1.56a	0.09a	10.22a	
UDP	65.2b	21.7b	13.6b	5.5a	1.30a	0.08a		8.18b
Pearson's correlation test among soil parameters								
Sand	1	-0.844**	-0.717**	-0.047*	0.249	-0.489**	-0.419*	-0.614**
Silt		1	0.370*	-0.004	-0.117	0.307*	0.317	0.465**
Clay			1	0.136	-0.451**	0.677**	0.414**	0.829**
pH				1	0.102	-0.124	-0.218	0.079
Bray1 P					1	-0.177	-0.117	-0.417**
OM						1	0.668**	0.733**
TN							1	0.501**

Means followed by the same letter in a column are not significantly different at the 0.05 probability Means followed by the same letter are not significantly different at the 0.05 probability level based on Duncan's multiple range test.

*, **Correlation is significant at 0.01 and 0.05 (Pearson).

Acronyms: OM: Organic matter; TN: Total nitrogen; CEC: Cation exchange capacity.

At the end of the growing season, a GPS device navigated to the center of each $4m^2$ plot. A handheld sickle was used to harvest rice paddy within the designated sampling areas. The harvested paddy was then threshed by hand, winnowed, and weighed. Subsequently, the grain was air-dried for approximately a day, and the grain moisture content was determined using the M3GTM (Dickey-john) moisture meter. The grain weight in kg per hectare was calculated using the following formula:

$$\text{Grain yield}\left(\text{kg ha}^{-1}\right)=\frac{\text{Grain yield}\left(\text{kg/net plot m}\right)*\left(10000\text{m/net plot m}\right)*\left(100\text{-measured grain mc\%}\right)}{\left(100\text{-14\% standard grain mc}\right)}$$

General Soil Characterization of Rice Production Zones

Surface (0 - 25 cm) soil surface samples of the 141 identified plots were collected from centers of all health plots delineated in farmer fields. Samples were air-dried, ground to pass a 2 mm sieve, and characterized. Particle size analysis was carried out using the pipette method [45]. A glass electrode measured soil pH in a 1:1 soil/water ratio. Organic carbon and total N were analyzed using a Leco Truspec C/N analyzer [46]. Plant available P was extracted with Bray1P solution using a 1:7 soil/solution ratio [47]. Exchangeable cations, calcium (Ca), magnesium (Mg), potassium (K), and sodium (Na), were extracted with neutral ammonium acetate (1 M NH_4OAC) [48]. The concentration of cations was analyzed using ICP - AES. Effective cation exchange capacity (ECEC) was estimated as the sum of exchangeable cations.

Yield Prediction and Mapping Based on Vegetation Indices

Estimating and yield mapping based on vegetation indices involved several crucial steps, as depicted in (Figure 3). They involved (1) acquisition and mosaicking of multispectral images acquired on a UAV platform, (2) extraction of NDVI VIs, (3) identification of yield plots based on NDVI reflectance data, and (4) rice yield assessment. With the objective to determine the optimal vegetation index for predicting rice grain yields in UDP and non-UDP fields, OSAVI emerged as the preferred yield predictor, exhibiting a relatively high correlation with grain yield

How to cite this article: Andrew M, Vincent Kodjo A, Thomas J, Ama Twumasi D, Amisu M. Spatial Analysis of UAS-generated Data to Evaluate Nitrogen Fertilizer Placement Alternatives, Predict and Map End-of-Season Rice Yield. Agri Res& Tech: Open Access J. 2024; 28(5): 556425. DOI: 10.19080/ARTOAJ.2024.28.556425

($r = 0.72$ $p < 0.05$) and the capability to address saturation issues at high reflectance, a concern associated with NDVI. Utilizing GIS-Pro, the Jenks Natural Breaks algorithm [49] was applied to categorize the OSAVI raster map of each farmer's field into four distinct, natural, and homogeneous groups. The aggregation and averaging of extrapolated yields of the four natural groups in each plot generated grain yields on the spatial scale.

Statistical Analyses

Relationships between soil parameters were evaluated using Pearson correlation analysis. Analysis of variance (ANOVA) was used to test yield differences, and mean separations were calculated using Tukey's studentized range with an alpha of 0.05 differences [50]. All data were checked for normality supported by a Shapiro-Wilk w statistic of 0.98 ($p = 0.05$) and a standard probability plot using the STATISTIX [51] software. The following two analytical procedures were used to evaluate and compare the plot and spatial yield data obtained from the study: (a) Box-and-whiskers analysis, a graphical representation of nonparametric ANOVA, to provide a visual summary of the central tendency, spread, and skewness of the data, and (b) descriptive statistics to identify trends and potential relation-ships between the variables.

Extrapolation of Plot Scale Yield to Spatial Field Scale

Following the outlined process illustrated in the flow chart in (Figure 3), grain yield data from $4m^2$ plots were extrapolated to encompass entire farmer field levels. Simple linear regression was developed between OSAVI and rice grain yields independently for plots in non-UDP and UDP fields. The models were used to extrapolate OSAVI values to their corresponding rice yields at the spatial scale. The projected yield values and the acreage within each class were utilized to calculate the kilograms of rice. The cumulative grain weight in the four natural break classes within a field determined the overall grain weight. Dividing this total weight by the entire field size yielded the average rice grain yield per hectare in the field.

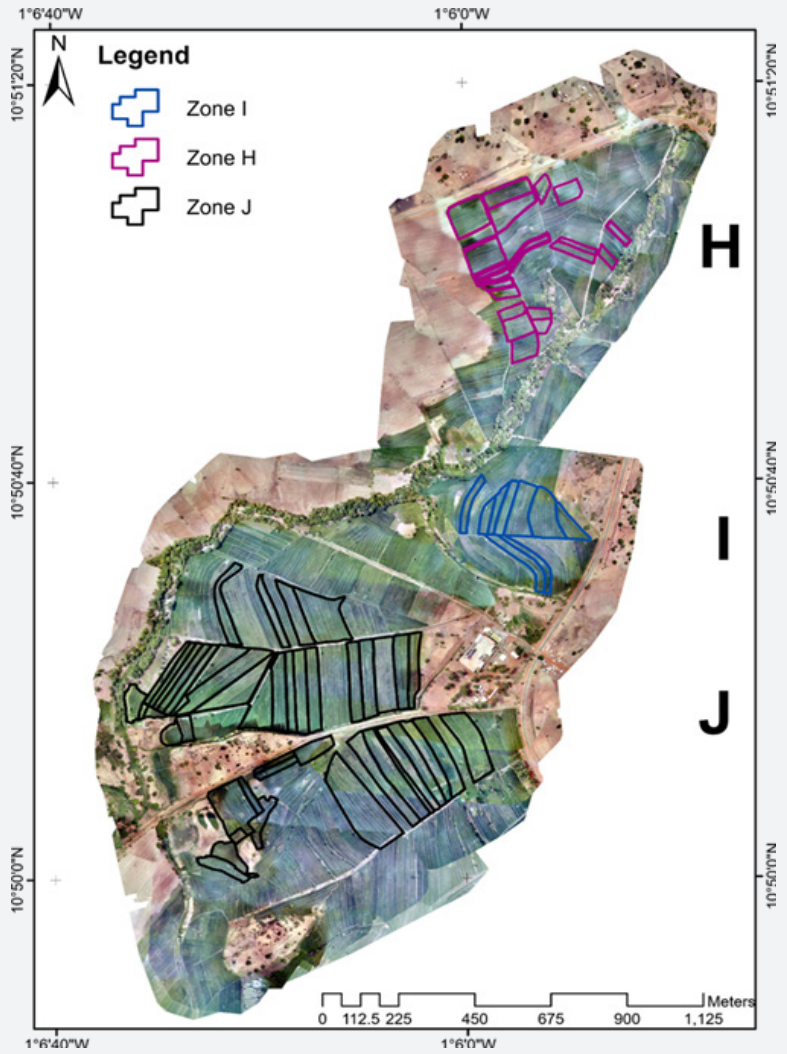

Figure 4: RGB Orthomosaic of the study site showing mapped-out farmer field boundaries in Zone H (purple boundaries), Zone I (blue boundaries) and Zone J (black boundaries).

How to cite this article: Andrew M, Vincent Kodjo A, Thomas J, Ama Twumasi D, Amisu M. Spatial Analysis of UAS-generated Data to Evaluate Nitrogen Fertilizer Placement Alternatives, Predict and Map End-of-Season Rice Yield. Agri Res& Tech: Open Access J. 2024; 28(5): 556425. DOI: 10.19080/ARTOAJ.2024.28.556425

Results

Orthomosaics and Crop Health Delineation

The RGB Orthomosaics for zones H, I, and J were created using imagery captured on the UAS platform. GPS coor-dinates marking field boundary points were employed to outline farmer fields in each zone (Figure 4). These true-color images are powerful tools that offer detailed, accurate, and easily interpretable information about rice fields. High spatial resolution, geo-referencing, and uniform scales enable precise measurements and analysis. Reflectance maps derived from orthomosaics for NDVI and OSAVI are illustrated in (Figures 5 and 6), respectively.

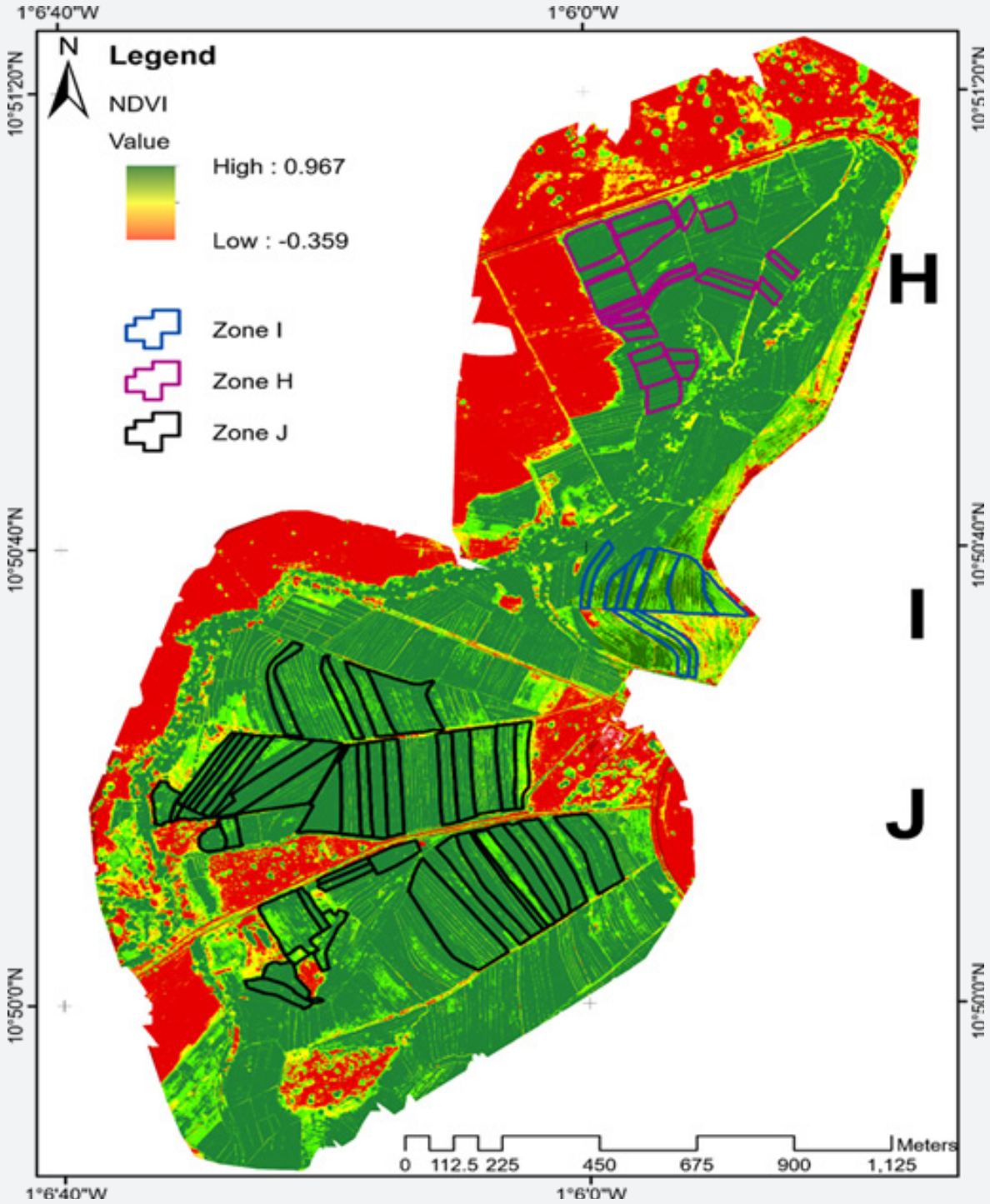

Figure 5: Reflectance maps of NDVI of individual farmer fields in Zones H, I, and J.

How to cite this article: Andrew M, Vincent Kodjo A, Thomas J, Ama Twumasi D, Amisu M. Spatial Analysis of UAS-generated Data to Evaluate Nitrogen Fertilizer Placement Alternatives, Predict and Map End-of-Season Rice Yield. Agri Res& Tech: Open Access J. 2024; 28(5): 556425. DOI: 10.19080/ARTOAJ.2024.28.556425

The NDVI reflectance map (Figure 5) is created using the formula developed by [39] to utilize satellite or UAS remote sensing data for monitoring vegetation health and density.

This map shows high NDVI values ranging from 0.6 to 0.9 as dark green areas, indicating dense and healthy vegetation. Moderate NDVI values (0.2 to 0.5) are displayed as light green to yellow areas. Low-health regions, characterized by pale green to almost yellowish areas, have NDVI values of less than 0.5. The OSAVI reflectance map (Figure 6), derived from the formula developed by [43], measures and monitors vegetation health, density, and coverage. High OSAVI values, represented by green colors, indicate dense and healthy vegetation. In contrast, lower values, shown in yellow, indicate sparse or stressed vegetation. Red colors on the OSA-VI map highlight areas of bare or exposed soil.

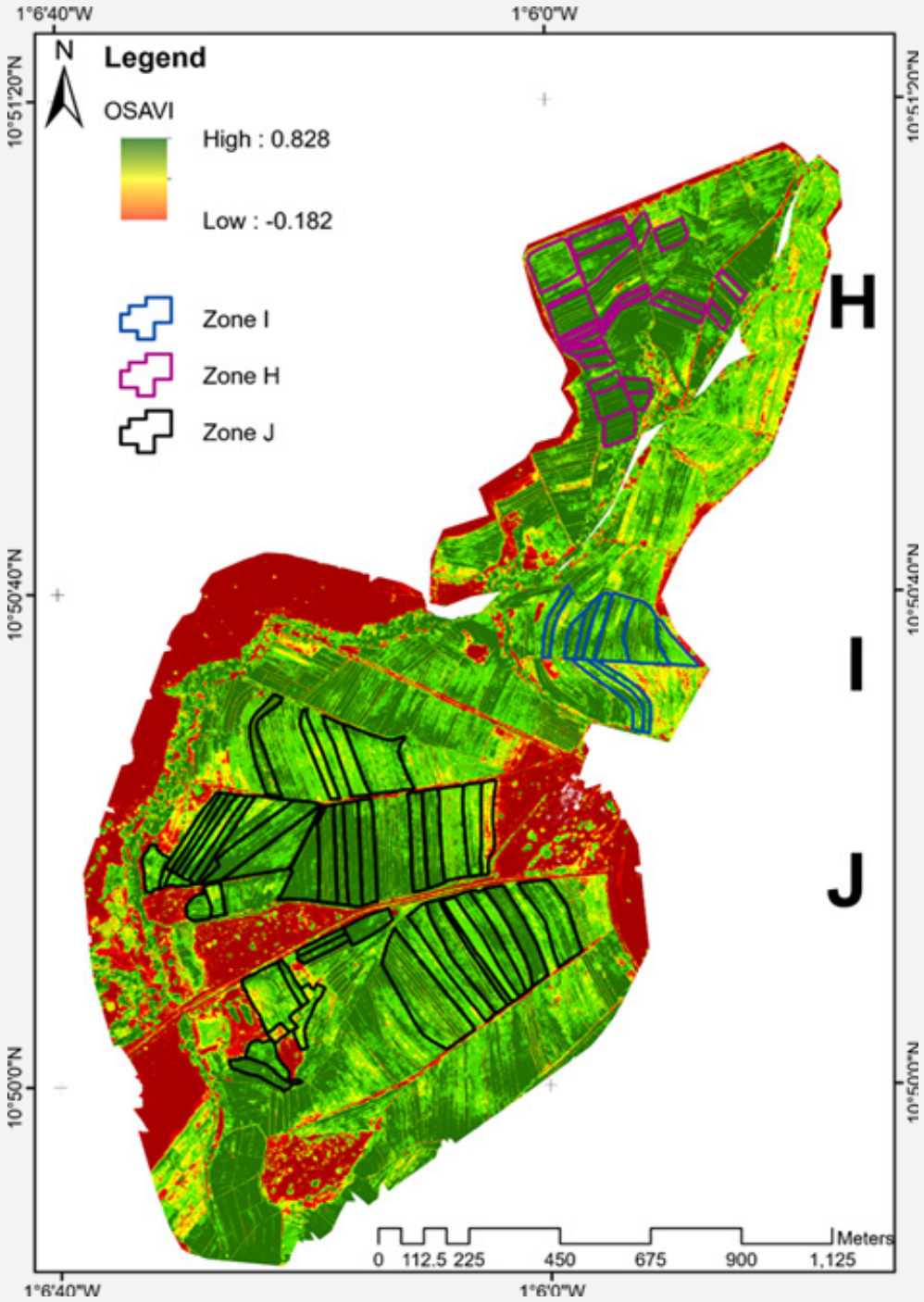

Figure 6: Reflectance maps of OSAVI of individual farmer fields in Zones H, I, and J.

How to cite this article: Andrew M, Vincent Kodjo A, Thomas J, Ama Twumasi D, Amisu M. Spatial Analysis of UAS-generated Data to Evaluate Nitrogen Fertilizer Placement Alternatives, Predict and Map End-of-Season Rice Yield. Agri Res& Tech: Open Access J. 2024; 28(5): 556425. DOI: 10.19080/ARTOAJ.2024.28.556425

Midseason Crop Health, N Management, and End-of-Season Rice Grain Yield

Figure 7 shows the relationships between the designated midseason crop health as a function of NDVI and OSAVI and the final rice grain yield obtained at the end of the season. There was a linear increase in yield from low $_{(OSAVI\ 0.544)}$ to high $_{(OSAVI\ 0.685)}$ health as assessed by OSAVI. On the other hand, no statistically significant differences in rice yields were observed between the medium $_{(NDVI\ 0.874)}$ and high $_{(NDVI\ 0.874)}$ crop health zones based on NDVI. However, medium and high-health zones had significantly higher yields than low $_{(NDVI\ 0.725)}$-health zones.

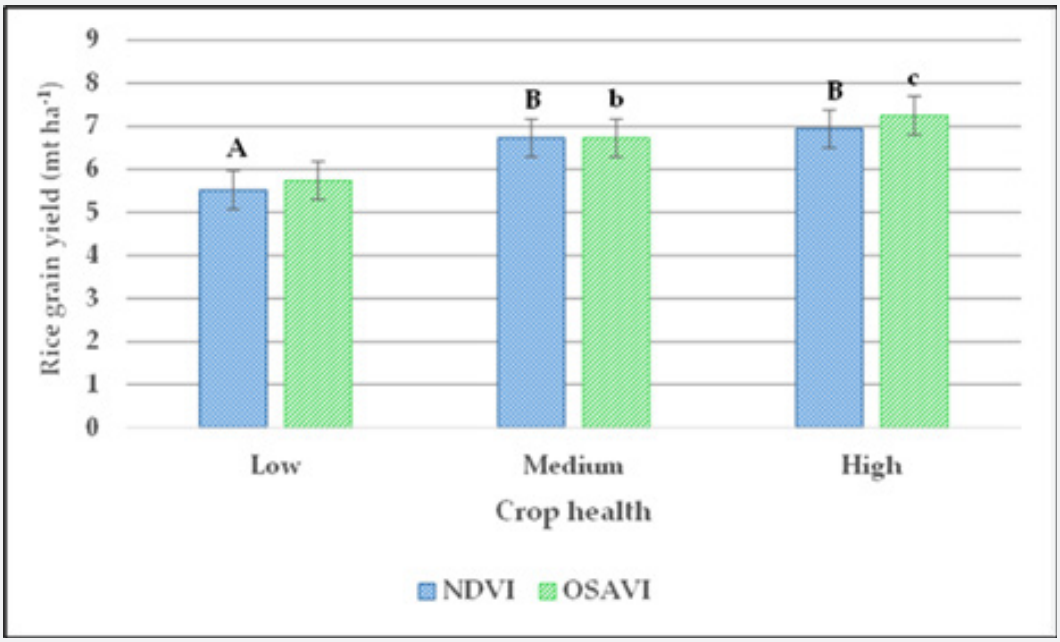

Figure 7: Relationships between crop health as assessed by NDVI and OSAVI and grain yields. Columns of the same color and the same letters are not significantly different. Mean separations were calculated using Tukey's stu-dentized range with an alpha of 0.05.

Soil Characterization

The upper layer of soil (0 - 25 cm) displays a prevalent sandy loam texture. Zone H exhibits the highest clay con-tent at 18.76% (Table 3). In contrast, Zone I shows the highest sand content at 70.6%, a considerably more significant proportion compared to zones H and J. Across all zones, the soil demonstrates acidity. While there is no notable difference in pH levels between zones, there is a slight increase from 5.4 in Zone H to 5.9 in Zone J. Zone H inherently has higher fertility levels than Zones I and J, as evidenced by elevated levels of organic matter (OM), total N, and cation exchange capacity (CEC). Particularly noteworthy is Zone J, which exhibits significantly higher concentrations of plant-available P, measuring 6.58 mg kg^{-1}, in contrast to 5.08 mg kg^{-1} and 2.32 mg kg^{-1} in Zones I and H, respectively.

Though initially not included in the research plan, soil properties have been naturally categorized into two groups based on N management systems, providing context for the study site background. Fields managed under UDP N revealed distinctive textural and fertility relationships. The UDP soils showed an average sand content of 65.2%, significantly higher than the 55% observed in non-UDP fields. In contrast, there was a reverse relationship in clay content, with non-UDP fields having a significantly higher percentage of clay (27.3%) than UDP fields (13.6%). While all soils had a sandy loam texture, the surfaces of fields under UDP management were noticeably coarser than their non-UDP counterparts, representing the sole distinctive fertility parameter between the two. The different N management systems could also be distinguished based on soil fertility. Non-UDP-managed fields exhibited a significantly higher CEC level of 10.22 compared to 8.18 cmol(+) kg^{-1} in UDP fields, as outlined in (Table 3).

Crop health assessment

The NDVI values used to define crop health categories in UDP and non-UDP fields are presented in (Table 4). These are based on reflectance values obtained from UAS data collected at the booting stage of the rice crop, as shown in (Figure 5).

Extrapolating Yields from Plot to Field Levels

The predictive equations for UDP and non-UDP fields are presented in (Figures 7a and 7b), respectively. These equations

How to cite this article: Andrew M, Vincent Kodjo A, Thomas J, Ama Twumasi D, Amisu M. Spatial Analysis of UAS-generated Data to Evaluate Nitrogen Fertilizer Placement Alternatives, Predict and Map End-of-Season Rice Yield. Agri Res& Tech: Open Access J. 2024; 28(5): 556425. DOI: 10.19080/ARTOAJ.2024.28.556425

reveal that OSAVI significantly predicts grain yield for UDP and non-UDP conditions, though the impact and the models' predictive power differs. The equations suggest that OSAVI significantly predicts rice grain yield, with 51.5% of the variability explained for UDP and 75.5% for non-UDP.

Plot and Spatial Scale Yield Analysis

A total of 141 yield data points were collected from NDVI crop health plots, with 68 points from UDP plots and 73 points (Table 5) from non-UDP plots. The data set was expanded to 324 yields (160 UDP and 131 non-UDP) points at the field level by applying spatial extrapolation using the Jenks natural breaks algorithm. At the plot scale, UDP plots' interquartile range (middle 50% of yields) ranged between 5.55 and 7.78 mt ha^{-1}, indicating a 2.23 mt ha^{-1} difference (Figure 9). Conversely, non-UDP fields exhibited a broader interquartile range of 2.66 mt ha^{-1}, with a minimum of 4.91 to a maximum of 7.57 mt ha^{-1}.

Table 4: Ranges of NDVI used for assigning crop health categories in UDP and non-UDP fields.

	UDP				Non-UDP			
Crop Health	**Min**	**Mean**	**Max**	**Std**	**Minimum**	**Mean**	**Maximum**	**Std**
Low	0.609	0.728	0.847	0.061	0.524	0.716	0.847	0.082
Medium	0.848	0.874	0.893	0.021	0.847	0.87	0.893	0.069
High	0.894	0.914	0.934	0.015	0.894	0.91	0.925	0.02

Table 5: Summary statistics of yield data from health plots and extrapolated spatial data of UDP and non-UDP fields.

N Management	Assessment points	Range	Minimum	Maximum	Median	Value	Std. deviation	Variance	CV (%)
Plot scale Assessment									
UDP	68	7.32	3.27	10.59	6.77	6.67	1.58	2.5	23.7
Non-UDP	73	7.99	1.92	9.91	6.03	6.14	1.82	2.3	29.61
Spatial scale Assessment									
UDP	160	2.4	6.32	8.72	7.38	7.37	0.49	0.24	6.67
Non-UDP	131	2.49	5.71	7.29	6.32	6.45	0.57	0.3	8.45

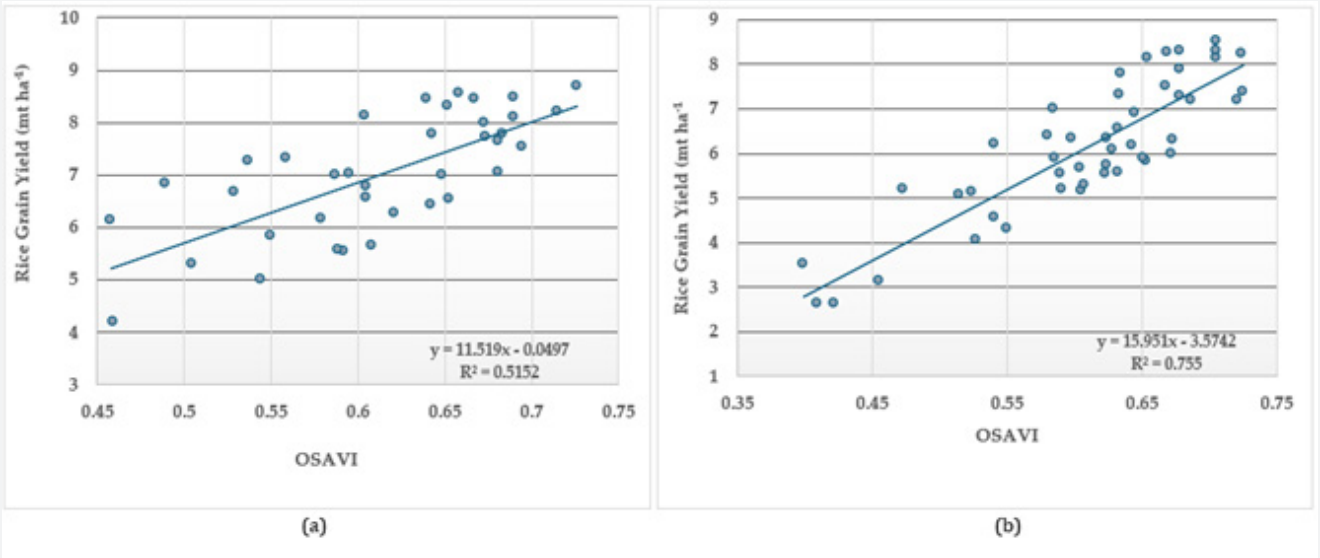

Figure 8: Linear regression of rice grain yield as a function of OSAVI (a) UDP and (b) non-UDP fields.

How to cite this article: Andrew M, Vincent Kodjo A, Thomas J, Ama Twumasi D, Amisu M. Spatial Analysis of UAS-generated Data to Evaluate Nitrogen Fertilizer Placement Alternatives, Predict and Map End-of-Season Rice Yield. Agri Res& Tech: Open Access J. 2024; 28(5): 556425. DOI: 10.19080/ARTOAJ.2024.28.556425

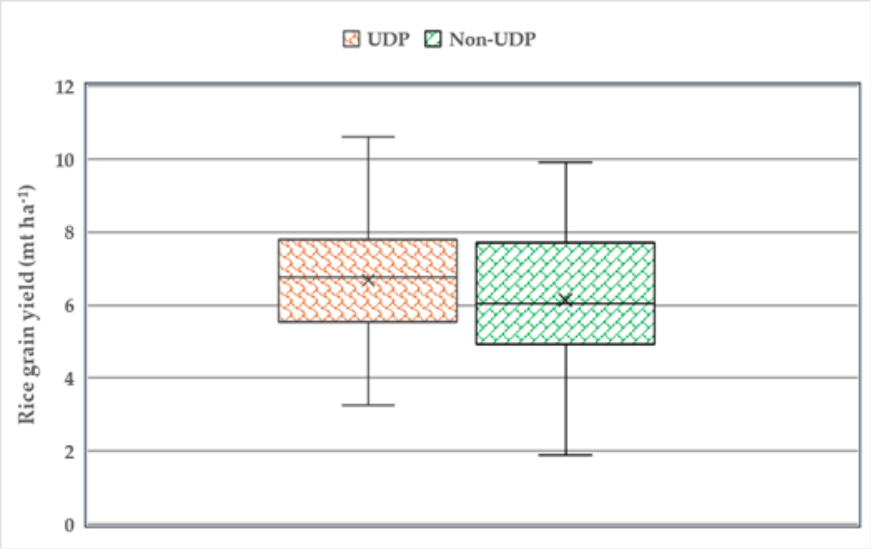

Figure 9: Box-and-whisker plot showing variation in rice grain yields (mt ha-1) under UDP (n = 68) and non-UDP (n = 73) N management plots. The figure also shows each N management system's median; Duncan means categories and upper.

The descriptive statistics (Table 5) revealed a yield range for UDP of 7.32 mt ha^{-1} with a minimum of 3.27 mt ha^{-1} and a maximum of 0.59 mt ha^{-1}, but non-UDP plots had a more extensive range of 7.99 mt ha^{-1} with a minimum of 1.92 mt ha^{-1} and a maximum of 9.91 mt ha^{-1}. The non-UDP plot yields were relatively more dispersed than their UDP counterparts. UDP plots' standard deviation (SD), variance, and coefficient of variation (CV) were 1.58, 2.50, and 23.7%, respectively. The non-UDP plot yields had an SD of 1.82, a variance of 3.30, and a CV of 29.61%. The average grain yield from UDP plots was 6.67 mt ha^{-1}, contrasting with 6.14 mt ha^{-1} in non-UDP plots (Figure 10). Tukey's HSD test indicates that the 11% difference is statistically significant at an alpha 0.05.

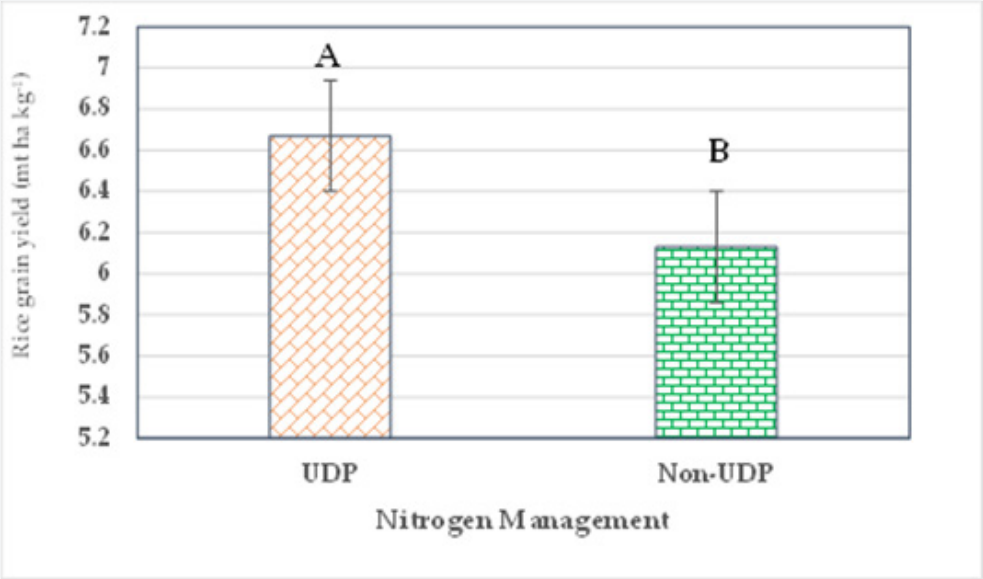

Figure 10: Comparative yield assessment of average rice grain yields from UDP and non-UDP plots. Bars with different letters significantly differ at 0.05 per Tukey's studentized test.

How to cite this article: Andrew M, Vincent Kodjo A, Thomas J, Ama Twumasi D, Amisu M. Spatial Analysis of UAS-generated Data to Evaluate Nitrogen Fertilizer Placement Alternatives, Predict and Map End-of-Season Rice Yield. Agri Res& Tech: Open Access J. 2024; 28(5): 556425. DOI: 10.19080/ARTOAJ.2024.28.556425

Field Scale Yield Analysis

In Figure 11, the interquartile range in the UDP fields was 0.70 mt ha^{-1}, ranging from 7.05 to 7.75 mt ha^{-1}, compared to the interquartile range of 1.07 mt ha^{-1} in the non-UDP data. The ranges in yields were substantially reduced in the field yield assessment (Table 5). It decreased by 4.92 mt kg^{-1} between UDP field and plot yields. A decrease of 5.5 kg ha^{-1} was observed in non-UDP management between plot and field-based assessments. The other dispersion variables also showed similar trends: SDs decreased by 1.58 mt ha^{-1} from plot to spatial field assessment under UDP management to 0.49 mt. ha^{-1} at the field scale, while non-UDP fields registered SDs of 1.82 mt ha^{-1} and 0.54 mt ha^{-1}, respectively. Variances and CVs showed the same decreasing trends from plot to field scales, as shown in (Table 5). There was a 17% reduction in CV in UDP plot scale yields to field scale level, while yield CV of non-UDP yield was reduced to 8.45% in non-UDP fields.

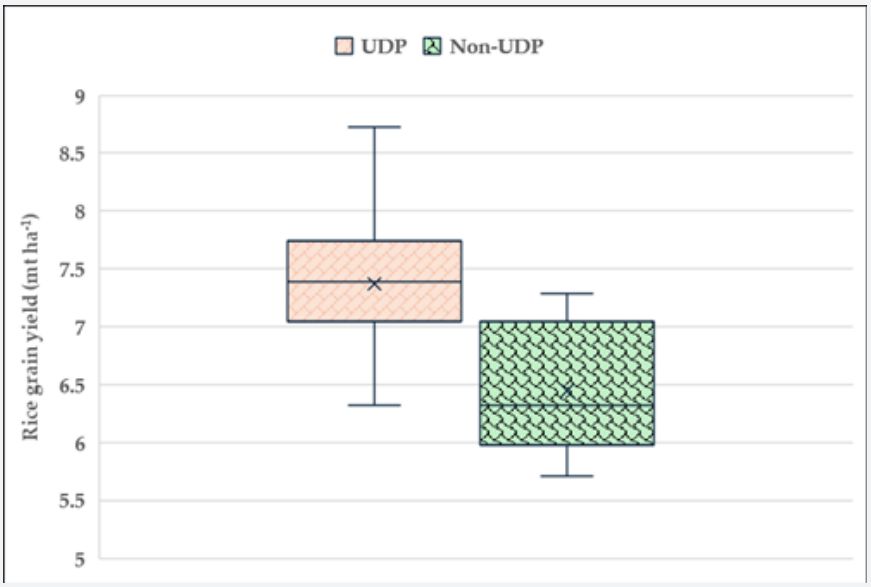

Figure 11: Box-and-whisker plot showing variation in rice grain yields (mt ha-1) under UDP (n = 160) and non-UDP (n = 131) N fields. The figure also shows each N management system's median; Duncan means categories and upper and lower quartiles.

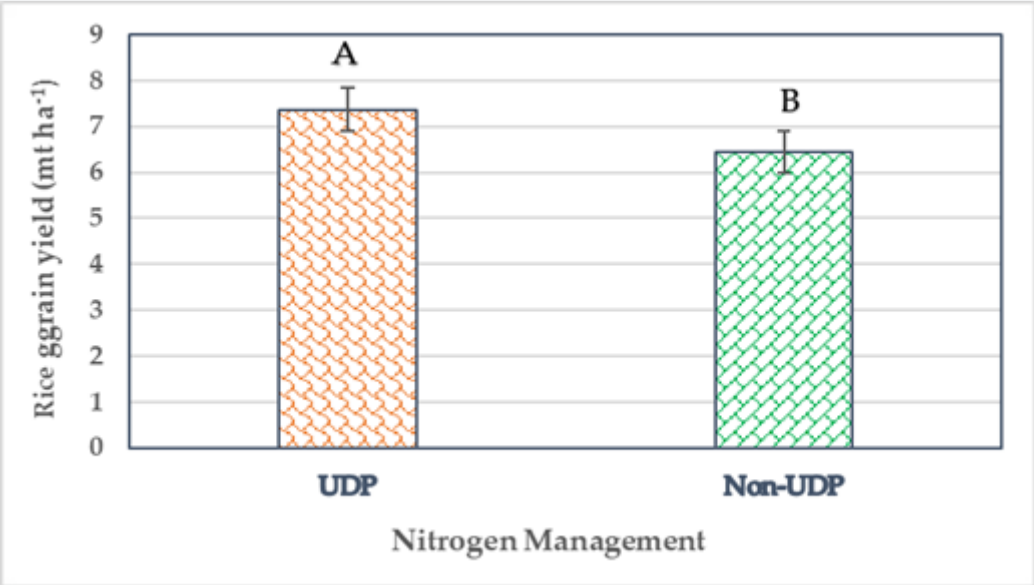

Figure 12: Grain yields in UDP and non-UDP farmers' fields. Bars with different letters significantly differ at 0.05 per Tukey's studentized test.

How to cite this article: Andrew M, Vincent Kodjo A, Thomas J, Ama Twumasi D, Amisu M. Spatial Analysis of UAS-generated Data to Evaluate Nitrogen Fertilizer Placement Alternatives, Predict and Map End-of-Season Rice Yield. Agri Res& Tech: Open Access J. 2024; 28(5): 556425. DOI: 10.19080/ARTOAJ.2024.28.556425

Scaling plot scale yields to spatial levels significantly reduced data variability. Initially, variances in plot scale da-ta for UDP and non-UDP were at 2.50 mt ha^{-1} and 3.30 mt ha^{-1}, respectively, which decreased to 0.24 mt ha^{-1} and 0.30 mt ha^{-1} at the farmer field level, as shown in (Table 5). Correspondingly, the coefficients of variation for UDP and non-UDP plot-scale data, initially at 23.07% and 29.96%, respectively, decreased to 6.7% and 8.45% at the farmer field scale. The calculated averages for rice grain yields in UDP and non-UDP fields were 7.37 mt ha^{-1} and 6.45 mt ha^{-1}, as depicted in (Figure 12). According to Tukey's standardized test, this 14% difference is statistically significant at the 0.05 level.

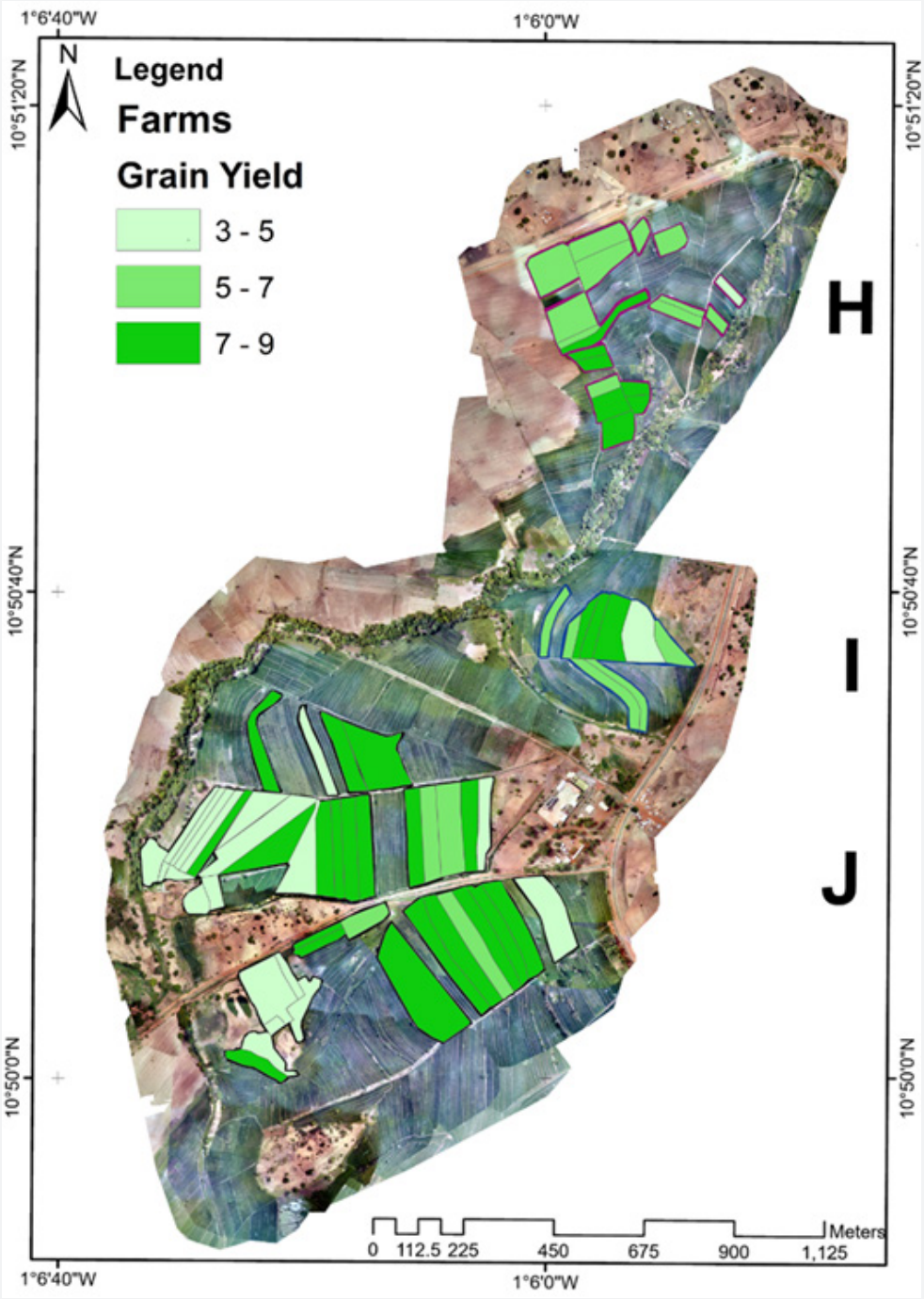

Figure 13: Predicted total rice grain yield in Zones H, I, and J producer fields as a function of N placement (UDP and non-UDP) systems.

How to cite this article: Andrew M, Vincent Kodjo A, Thomas J, Ama Twumasi D, Amisu M. Spatial Analysis of UAS-generated Data to Evaluate Nitrogen Fertilizer Placement Alternatives, Predict and Map End-of-Season Rice Yield. Agri Res& Tech: Open Access J. 2024; 28(5): 556425. DOI: 10.19080/ARTOAJ.2024.28.556425

Rice Grain Yield Mapping

An important outcome of this research is the generation of high-resolution prediction digital maps illustrating the landscape patterns of rice production in the three zones (Figure 13). These rice grain yield maps are characterized by their high spatial resolution, geo-referencing, and uniform scales, which enable precise measurements and analysis. The scale of these maps allows for identifying field boundaries and other pertinent field features, providing a comprehensive overview of rice grain yield potential across the three intervention zones [62]. It also facilitates precise management and planning. Zone J has a notably higher average grain yield, achieving 7.17 mt ha^{-1} under UDP management compared to 6.42 mt ha^{-1} non-under UDP management (Table 6).

Table 6: Summary of rice productivity in Zones H, I, and J as a function of N management as assessed based on predicted yield data.

Zone	UDP	Non-UDP
Average grain yield		
H	6.7ab†	5.95a
I	6.22b	5.82a
J	7.17a	6.42a

†Means followed by the same letter in a column are not significantly different at the 0.05 probability level based on Duncan's multiple range test.

Discussion

The results of the physicochemical analysis affirmed the variable and depleted nature of soils in the study zone. These results support the claim by [52,53] that soil fertility poses a significant challenge to agricultural production in the West African Savanna. The low P content and organic matter levels agree with the findings of [54], who reported soils' low overall fertility status in the Tono irrigation scheme.

In this study, UAS technology was utilized to evaluate the impact of different N placement strategies on rice grain yield. The rationale for employing this aerial assessment method is diverse. Still, the primary advantages include: (1) UAS captures high-resolution images that offer detailed spatial information, allowing for precise assessment of N distribution and crop health [36]. (2) The system detects small-scale variability within fields, enhancing the understanding of N placement effectiveness [55] and enabling the prediction and mapping of rice yields [56], a critical objective of this study. (3) The multispectral imaging capabilities of the UAS system permit the calculation of indices such as NDVI and OSAVI, which are sensitive to N status and plant health. (4) Additionally, UAS technology reduces the need for extensive manual labor in data collection [57] because it covers large fields at a time [58].

According to [59], the booting stage of the rice crop at which the aerial survey was carried out marks the rice plant's nutrient growth peak, featuring the highest leaf area index. The high leaf area index reflects the plant's maximal photosynthetic capacity and yield potential [60], pertinent to one of the addressed objectives. Orthomosaics from the captured imagery depicted rice fields in the three intervention zones. These orthomosaics rectify heights, tilts, topographic relief, and lens distortions, ensuring geometric accuracy [61]. The high spatial resolution, geo-referencing, and uniform scales of the map enable precise measurements and analysis [62]. NDVI raster maps derived from these orthomosaics facilitated the identification of crop health plots as a function of UDP and non-UDP. The categorized NDVI means for UDP fields are 0.728 for low health, 0.874 for medium health, and 0.914 for high health. The non-UDP mean crop health equivalents were 0.716 for low, 0.870 for medium, and 0.910 for high health plots. In a previous study, [63] mapped rice crop health using NDVI ranges, defining very good health as 0.721 - 0.920, good health as 0.421 - 0.720, normal health as 0.221 – 0.42, and poor health as 0.110 - 0.220.

The end-of-season assessment of rice grain yield significantly correlated with assigned crop health ($r = 0.68$, significant at $p<0.05$). However, this correlation weakened at elevated NDVI levels. This finding aligns with [64], who observed a non-linear relationship among NDVI, crop health, and end-of-season yields. According to [65], NDVI tends to saturate asymptotically with increasing reflectance in dense canopies, leading to the underestimation of rice yields in areas with high vegetative growth, as observed by [66]. Nevertheless, this study demonstrated that NDVI remained sensitive enough to differentiate crop health areas and was a distinguishing metric between N management systems.

In contrast, OSAVI exhibited a consistent linear relationship ($r = 0.72$ significant at $p<0.05$) with crop health throughout the spectrum, as noted by [67]. This vegetation index then functioned as a proxy for forecasting end-of-season rice grain yields based on mid-season reflectance. Consequently, akin to a prior study where [68] employed linear regression models to forecast rice yield using OSAVI, we leveraged the linear correlation association between OSAVI derived from a single midseason reflectance assessment to extrapolate plot-scale rice yields to spatial dimensions.

In this study, the innovative integration of multiple vegetation indices, NDVI and OSAVI, epitomizes the frontier of agricultural monitoring and management. NDVI is renowned for identifying crop health through sensitivity to vegetation density, chlorophyll concentration, and vigor. OSAVI is also distinguished by its robustness in reducing soil background effects. In comparing multiple vegetation indices for rice yield estimation, OSAVI [69,70] had a slightly better correlation with rice yield than NDVI, especially in areas with low vegetation. The soil adjustment factor in OSAVI helped reduce the noise caused by soil reflectance, leading to more accurate yield prediction. A simi-lar study in Southeast Asia [71] suggested that NDVI and OSAVI provide more stable and reliable predictions in heterogeneous fields with varying soil conditions. In this study, the creative use of NDVI and

How to cite this article: Andrew M, Vincent Kodjo A, Thomas J, Ama Twumasi D, Amisu M. Spatial Analysis of UAS-generated Data to Evaluate Nitrogen Fertilizer Placement Alternatives, Predict and Map End-of-Season Rice Yield. Agri Res& Tech: Open Access J. 2024; 28(5): 556425. DOI: 10.19080/ARTOAJ.2024.28.556425

OSAVI leverages the strengths of each index: NDVI for real-time crop health monitoring and OSAVI for accurate yield predictions.

This study also leveraged the innovative computational capabilities of the Jenks natural breaks classification algorithm [49] to optimize the classification of OSAVI values from rice plots, thereby enhancing yield predictions and their extrapolation to spatial dimensions. Renowned for its robustness in handling spatial data distribution, this classification system effectively organizes data into distinct classes, minimizing variances within classes while maximizing differences between them, as noted by [72]. This ensures that the classification reflects true natural groupings within the data [73], highlighting the algorithm's utility in capturing yield variation and emphasizing its value in agricultural planning and management. [74] used this method to classify crop yields and found it superior to other classification methods in terms of accurately reflecting the spatial variability of crop yields. Using this classification system on the high-resolution data captured by UAS technology, the accuracy and variability of predicted rice grain yields were significantly enhanced, leading to improved data interpretation and visualization, as illustrated in (Figure 12).

Linear regressions were established between OSAVI and rice yield as a function of N placement. The coefficients of determination, R2 for the prediction equations, were 0.5152 and 0.7555 for UDP and non-UDP plots, respectively. The aggregation of extrapolated yields in the four Jenks grouping of each field constituted the potential or predicted rice grain yield for the entire field on the spatial scale. This approach allowed for the prediction, subsequent mapping, and generation of a realistic, spatially meaningful predicted potential rice yield map for the intervention zones. This visual tool can be essential to policymakers, researchers, and farmers, helping them quickly grasp complex spatial data and make informed decisions before the end of the growing season. As highlighted by [75], the assessment scale is crucial in determining crop yield variability. Establishing a connection between plot-scale data and extrapolated spatial data is also essential for comprehending and predicting trends, patterns, and variations in crop yields within fields. Additionally, considering yield variability at multiple scales is pertinent for modeling, predicting, and mapping, a key study objective for this study.

Following the recommendation of [76], we utilized summary statistics and the box-and-whisker plot, a graphical representation depicting the distribution of a dataset. This approach effectively illustrated the significant dependence of yield variability on the evaluation scale. Two significant observations were made regarding grain yield structure and metrics at the plot and spatial data levels. Firstly, it was noted that the relationships among different metrics remained relatively consistent with those observed in the analysis of plot-scale yields. Secondly, the transition from plot-scale data to spatial levels substantially reduced data variability and enhanced data quality. It improved the data's discriminatory capacity between N placement alternatives on rice yield, which is the second primary objective of the study.

While data generated at both plot and spatial scales exhibited the same relationships and trends, the upscaling process refined the assessment data by reducing standard deviations, variance, and coefficients of variation (CVs). As indicated by [77], the success of spatial assessment hinges on the size and total number of samples. In this study, augmenting the sample size from 141 plot yields (68 UDP and 73 non-UDP plots) (Table 5) to 291 (160 UDP and 131 non-UDP) (Table 6) following the Jenks natural breaks grouping led to an improved data distribution and enhanced discrimination assessment of N placement alternatives.

On UDP plots, grain yields ranged from a minimum of 3.27 to a maximum of 10.59 mt ha^{-1} with a range of 7.32 mt ha^{-1} but narrowed to a minimum yield of 6.32 to a maximum of 8.72mt ha^{-1}, a range of 2.4 mt ha^{-1} at the spatial scale. Grain yield from UDP plots exceeded their non-UDP counterparts by 0.69%, and at the field scale, UDP outperformed non-UDP by 0.84%. Similar relationships were obtained by [78,79] in their rice yield-N placement strategies investigations in Northern Ghana and Southern Bangladesh, respectively.

The research produced accurate data and utilized straightforward spatial analysis to illustrate, predict, and map the end-of-season rice grain yield. The maps illustrate rice yield's spatial distribution and variability across the three intervention zones, providing insights into landscape-level production patterns. The maps are created with high spatial resolution, allowing detailed visualization of yield patterns across the landscape. These not only facilitate a detailed examination of the spatial variability in rice yield but also support targeted agricultural interventions and re-source management by highlighting areas with different yield potentials. A thorough examination of the anticipated yield chart (Figure 12), corroborated by a yield analysis (Table 6), revealed that zone J possessed the highest yield potential, averaging 7.17 metric tons per hectare. This yield is notably superior compared to zones H and I.

The observed yield distribution projected by the study corresponds with the soil fertility patterns noted during the initial physicochemical assessment of the project area. The P content was prominent among the fertility indicators, affecting the rice grain yield after fulfilling the N requirement. This finding echoes a similar study conducted in Pakistan [80], where applying 90 kilograms of P205 led to a 29% increase in paddy rice yield compared to the control once the N levels were adequate. Furthermore, Pearson correlation analysis demonstrated a significant link between P and rice grain yield (r = 0.74, significant at 0.05). In contrast, the high sand content (70.6%) in Zone I is likely re-sponsible for the reduced grain yield observed, which could adversely affect the soil's water and nutrient dynamics.

How to cite this article: Andrew M, Vincent Kodjo A, Thomas J, Ama Twumasi D, Amisu M. Spatial Analysis of UAS-generated Data to Evaluate Nitrogen Fertilizer Placement Alternatives, Predict and Map End-of-Season Rice Yield. Agri Res& Tech: Open Access J. 2024; 28(5): 556425. DOI: 10.19080/ARTOAJ.2024.28.556425

Conclusion

This study employed Unmanned Aerial System (UAS)-derived data to create reflectance orthomosaics of NDVI and OSAVI. at the booting stage of the rice crop. Three progressive health plots were identified in UDP and non-UDP N placement rice fields using NDVI. While a linear correlation was observed between NDVI and crop health, its relationship with end-of-season rice grain yield was nonlinear. In contrast, OSAVI exhibited linear correlations with crop health and end-of-year yields, establishing it as the preferred end-of-season yield predictor. In addition, OSAVI provided more suitable and reliable predictions in heterogeneous fields with varying soil conditions and was therefore utilized as a suitable index to extrapolate plot yield data to spatial dimensions through linear regression.

The OSAVI data in the linear equation were generated from distinct natural homogeneous groups identified by the Jenks natural breaks algorithm for each farmer's field. Aggregating the four natural break yields constituted the predicted average rice yield for the respective field, generating spatially meaningful predicted yields for each zone. This process produced a high-resolution, practical digital spatial yield map depicting rice distribution and productivity for each zone. The yield data analysis from plot-level and spatial scale assessments involved summary statistics and plot-scale analyses. Although yields from both scales demonstrated similar relationships and trends, upscaling plot data to spatial dimensions refined the assessment data by reducing standard deviations, variances, and coefficients of variation.

Assessing the impact of N placement at the plot scale highlighted the superiority of UDP-N placement over non-UDP N management by 9.9%, equivalent to 0.6 mt ha^{-1}. In spatial assessment data, UDP field yields surpassed on-UDP counterparts, outperforming non-UDP by 14.3%, resulting in a yield differential of 0.92 mt ha^{-1}. This research has developed a concrete protocol for predicting and producing high-resolution maps of rice yield, which can be analogous to field mapping, utilizing midseason crop reflectance data generated from the UAS technology.

Acknowledgments

We express our deepest gratitude to Mr. Jeff DaCosta Osei and Mr. Prosper Kpiebaya for their invaluable assistance with the GIS work crucial to producing the images for this research. Their expertise and dedication significantly contributed to the quality and success of this study.

References

1. MiDA (Millennium Development Authority) (2010) Investment opportunity in Ghana: Maize, Rice, and Soybean. Accra, Ghana: MiDA.
2. Osei-Asare Y (2010) Mapping of poverty reduction strategies and policies related to rice development in Ghana. Nairobi, Kenya: Coalition for African Rice Development (CARD).
3. Bannor RK (2015) Long-run and short-run causality of rice consumption by urbanization and in-come growth in Ghana. ACADEMICIA: An Int Multidiscip Res J 5(2): 173-189.
4. Ministry of Food Agriculture (MoFA) (2021) Agriculture in Ghana: Facts and Figures (2012). Statis-tics, Research and Information Directorate (SRID). Accra p. 1-45.
5. Denkyirah EK, Aziz AA, Nketiah OO, Okoffo ED (2016) Access to credit and constraint analysis: the case of smallholder rice farmers in Ghana. J AgricStudies 4(2): 53-72.
6. Becker M, Johnson D (2001) Cropping intensity effects on upland rice yield and sustainability in West Africa. Nutrient Cycling in Agroecosystems 59: 107-11.
7. Abe SS, Buri MM, Issaka RN, Kiepe P, Wakatsuki T (2010) Soil fertility potential for rice production in West African lowlands. JARQ 44(4): 343-355.
8. Balasubramanian V, Sie M, Hijmans RJ, Otsuka K (2007) Increasing Rice Production in Sub-Saharan Africa: Challenges and Opportunities. Adv Agronom 94(06): 55-133.
9. Olaf K, Emmanuel D (2009) Global food security response: Ghana rice study. Attachment I to the Global Food Security Response West African Rice Value Chain Analysis.
10. Aker JC, Block S, Ramachandran V, Timmer CP (2010) West African experience with the world rice crisis, 2007-2008. The rice crisis: markets, policies and food security pp. 143-162.
11. Lançon F, Ehrenstein O (2002) Potential prospects for rice production in West Africa. In Sub-regional workshop on harmonization of policies and coordination of programs on rice in the ECOWAS sub-region Accra, Ghana p. 5-6.
12. Cong XH, Shi FZ, Ruan XM, Luo YX, Ma TC, et al. (2017) Effects of nitrogen fertilizer application rate on nitrogen use efficiency and grain yield and quality of different rice varieties. J Appl Ecol 28(4): 1219-1226.
13. Ladha JK, Pathak H, Krupnick TJ, Six J, Van Kessel C (2005) Efficiency of fertilizer nitrogen in cereal production: retrospect and prospects. Adv Agron 87: 85-156.
14. Alam MM, Karim MR, Ladha JK (2013) Integrating best management practices for rice with farmers' crop management techniques: A potential option for minimizing rice yield gap. Field Crops Res 144: 62-68.
15. Dong NM, Brandt KK, Sørensen J, Hung NN, Hach CV, et al. (2012) Effects of alternating wetting and drying versus continuous flooding on fertilizer nitrogen fate in rice fields in the Mekong Delta, Vietnam. Soil Biology Biochem 47: 16-174.
16. IFDC (International Fertilizer Development Center) (2013) Fertilizer deep placement. IFDC solutions. IFDC, Muscle Shoals, AL.
17. Savant NK, Stangel PJ (1990) Deep placement of urea super granules in transplanted rice: Principles and practices. Fertilizer Research 25: 1-83.
18. Rochette P, Angers DA, Chantigny MH, Gasser MO, MacDonald JD, et al. (2013) Ammonia Volatilization and Nitrogen Retention: How Deep to Incorporate Urea. J Environ Qualit 42(6): 1635-1642.
19. Yao Y, Zhang M, Tian Y, Zhao M, Zhang B, et al. (2018) Urea deep placement for minimizing NH3 loss in an intensive rice cropping system. Field Crops Res 218: 254-256.
20. Huda A, Gaihre YK, Islam MR, Singh U, Islam MR, et al. (2016) Floodwater ammonium, nitrogen use efficiency and rice yields with fertilizer deep placement and alternate wetting and drying under triple rice cropping systems. Nutrient Cycling Agroecosyst 104: 53-66.

How to cite this article: Andrew M, Vincent Kodjo A, Thomas J, Ama Twumasi D, Amisu M. Spatial Analysis of UAS-generated Data to Evaluate Nitrogen Fertilizer Placement Alternatives, Predict and Map End-of-Season Rice Yield. Agri Res& Tech: Open Access J. 2024; 28(5): 556425. DOI: 10.19080/ARTOAJ.2024.28.556425

21. Pasandaran E, Gultom B, Adiningsih JS, Apsari H, Rochayati S (1998) Government poli-cy support for technology promotion and adoption: a case study of urea tablet technology in Indone-sia. Nutrient Cycling Agroecosystems 53(1): 113-119.

22. Azumah Shaibu A, William A (2017) Effect of Urea Deep Placement Technology Adoption on the Production Frontier: Evidence from Irrigation Rice Farmers in the Northern Region of Ghana. Int J Biol Biomol Agric Food Biotech Engineer 11(4).

23. Liverpool-Tasie LSO, Adjognon S, Kuku-Shittu O (2015) Productivity effects of sustainable intensification: The case of Urea deep placement for rice production in Niger State, Nigeria. Afr J Agric Resour Econom 10(1): 51-63.

24. Bandaogo A, Bidjokazo F, Youl S, Ebenezer S, Robert A, et al. (2015) Effect of fertilizer deep placement with urea supergranule on nitrogen use efficiency of irrigated rice in Sourou Valley (Burkina Faso). Nutr Cycl Agroecosyst 102: 79-89.

25. Mosleh MK, Hassan QK, Chowdhury EH (2016) Development of a remote sensing-based rice yield forecasting model. Spanish J Agri Res 14(3): 1-11.

26. Stafford JV (2000) Implementing Precision Agriculture in the 21st Century, 2002. J Agric Engineer Rese 76(3): 267-275.

27. Wang YP, Chang KW, Chen RK, Lo JC, Shen Y (2010) Large-area rice yield forecasting using satellite imageries. Int J Appl Earth Observ Geoinfo 12(1): 27-35.

28. Wakamori K, Ichikawa D, Oguri N (2017) Estimation of rice growth status, protein content and yield prediction using multi-satellite data," 2017 IEEE International Geoscience and Remote Sensing Sym-posium (IGARSS), Fort Worth, TX, USA pp. 5089-5092.

29. Nuarsa IW, Nishio F, Hongo C (2012) Rice yield estimation using Landsat ETM+ data and field observation. J Agric Sci 4(3): 45.

30. Emmanouil P, Nicholas D, Nicolas RD, Nikolaos V (2016) Spyropoulos, "The role of spatial and spectral resolution on the effectiveness of satellite-based vegetation indices," Proc. SPIE 9998, Remote Sensing for Agriculture, Ecosystems, and Hydrology XVIII, 99981L.

31. Mulla DJ (2013) Twenty-five years of remote sensing in precision agriculture: Key advances and remaining knowledge gaps. Biosyst Engineer 4(114): 358-371.

32. Abuzar M, Sheffield K, Whitfield D, O'Connell M, McAllister A (2014) Comparing inter-sensor NDVI for the analysis of horticulture crops in south-eastern Australia. Ame J Remote Sensing 2(1): 1-9.

33. Khan Z, Rahimi-Eichi V, Haefele S, Garnett T, Miklavcic SJ (2018) Estimation of vegetation indices for high-throughput phenotyping of wheat using aerial imaging. Plant Methods 14: 1-11.

34. Ozdogan Mutlu, Yang, George Allez, Chelsea C (2010) Remote Sensing of Irrigated Agriculture: Opportunities and Challenges. Remote Sensing 2(9): 2274-2304.

35. Cammarano Davide, Hainie Zha, Lucy Wilson, Yue Li, William D (2020) A Remote Sensing-Based Approach to Management Zone Delineation in Small Scale Farming Systems. Agronomy 10(11): 1767.

36. Zhang CH, Kovacs JM (2012) The Application of Small Unmanned Aerial Systems for Precision Agriculture: A Review. Precision Agric 13(6): 693-712.

37. Chapman SC, Merz T, Chan A, Jakeway P, Hrabar S, et al. (2014) Pheno-copter: a low-altitude, autonomous, remote-sensing robotic helicopter for high-throughput field-based phenotyping. Agronom 4(2): 279-301.

38. Schirrmann M, Giebel A, Gleiniger F, Pflanz M, Lentschke J, et al. (2016a) Monitor-ing agronomic parameters of winter wheat crops with low-cost UAV imagery. Remote Sensing 8: 706.

39. Rouse JW, Haas RH, Schell JA, Deering DW (1973) Monitoring the vernal advancements and retrogradation of natural vegetation. NASA/GSFC Final Report, Greenbelt, MD, USA.

40. Blackmer TM, Schepers JS, Varvel GE, Walter-Shea EA (1996) Nitrogen deficiency detection using reflected shortwave radiation from irrigated corn canopies. Agron J 88: 1-5.

41. Stone ML, Solie JB, Raun WR, Whitney RW, Taylor SL, et al. (1996) Use of spectral radiance for correcting in-season fertilizer nitrogen deficiencies in winter wheat. Trans. Am Soc Agric Eng 39: 162.

42. Hatfield JL, Kanemasu ET, Asrar G, Jackson RD; Pinter PJ, et al. (1985) Leaf-area estimates from spectral measurements over various planting dates of wheat. Int J Remote Sensing 6(1): 167-175.

43. Rondeaux G, Steven M, Baret F (1996) Optimization of Soil-adjusted vegetation indices. Remote Sens Environ 55: 55-107.

44. Sensefly (2016) High-performance fixed-wing mapping drones. eBee: sensefly S.A.

45. Walter NF, Hallberg GR, Fenton TS (1978) Particle size analysis by the Iowa State Univer-sity Soil Survey Lab. Standard procedures for evaluation of quaternary materials in Iowa. Iowa Geo-logical Survey, Iowa City pp. 61-74.

46. Combs SM, Nathan MV (1998) Soil organic matter. p. 53–58. In Comun Soil Sci. Plant Anal. 22: 159–168. Recommended chemical soil test procedures for the north-central Sikora, Lujan D.E. Stott. 1996. Soil organic carbon and nitrogen. P. 157–168. In J.W. Doran and A.J. Jones (ed.) Methods for as-region. North Central Regional Res. Publ. No. 221 (revised). Assessing soil quality. SSSA Spec. Publ. 49. SSSA, Madison, Missouri Agric. Exp. Sta. SB 1001, Columbia, MO.

47. Bray RH, Kurtz LT (1945) Determination of Total Organic and Available Forms of Phospho-rus in Soils. Soil Sci 59: 39-45.

48. Warncke D, Brown JR (1998) Potassium and other basic cations. Recommended chemical soil test procedures for the North Central Region 1001: 31-33.

49. Jenks GF (1967) The data model concept in statistical mapping. Int Yearb Cartogr 7(1): 186-190.

50. SAS Institute Inc (2018) SAS/STAT® 15.1 User's Guide. Cary, NC: SAS Institute Inc.

51. Statistix 9 (2019)Tallahassee FL, USA.

52. Konja TF, Mabe FN, Alhassan H (2019) Technical and resource-use-efficiency among small-holder rice farmers in Northern Ghana, Cogent Food Agric 5: 1.

53. Bationo A, Fening JO, Kwaw A (2018) Assessment of soil fertility status and integrated soil fertility management in Ghana. In: Improving the profitability, sustainability, and efficiency of nu-trients through site-specific fertilizer recommendations in West Africa agroecosystems. Springer, Cham pp. 93-138.

54. Gyekye PM, Domozoro CYF, Musah M, Ababio FO, Sadick A (2021) Soil and Land Suita-bility Assessment for Rice Cultivation at Tono Irrigation Area in the Upper East Region, Ghana. Open J Appl Sci 11: 1230-1239.

55. Bendig J, Bolten A, Bennertz S, Broscheit J, Eichfuss S, et al. (2015) Combining UAV-based plant height from crop surface models, visible, and near-infrared vegetation indices for bio-mass monitoring in barley. Int J Applied Earth Observation Geoinfo 39: 79-87.

56. Bo Li, Xiangming Xu, Li Zhang, Jiwan Han, Chunsong Bian, et al. (2020) Above-ground biomass estimation and yield prediction in potato by using UAV-based RGB and hyperspectral imaging. ISPRS J 162: 161-172.

57. Mulla DJ (2013) Twenty-five years of remote sensing in precision agriculture: Key advances and remaining knowledge gaps. Biosystems Engineering 114(4): 358-371.

How to cite this article: Andrew M, Vincent Kodjo A, Thomas J, Ama Twumasi D, Amisu M. Spatial Analysis of UAS-generated Data to Evaluate Nitrogen Fertilizer Placement Alternatives, Predict and Map End-of-Season Rice Yield. Agri Res& Tech: Open Access J. 2024; 28(5): 556425. DOI: 10.19080/ARTOAJ.2024.28.556425

58. Zhang C, Kovacs JM (2012) The application of small unmanned aerial systems for precision agriculture: a review. Precision agriculture 13: 693-712.

59. Yuan N, Gong Y, Fang S, Liu Y, Duan B, et al. (2021) UAV remote sensing estimation of rice yield based on adaptive spectral end members and bilinear mixing model. Remote Sensing 13(11): 2190.

60. Hobbs T (1995) The use of NOAA-AVHRR NDVI data to assess herbage production in the arid range-lands of Central Australia. Int. J Remote Sens 16(7):1289-1302.

61. Jenks GF, Caspall FC (1971) Error on choroplethic maps: definition, measurement, reduction. Ann Assoc Am Geogr 61(2): 217-244.

62. Longley PA, Goodchild MF, Maguire DJ, Rhind DW (2015) Geographic Information Sys-tems and Science (4th ed.). Wiley.

63. Marsujitullah DAK, Manggau FX (2023) Health Analysis of Rice Plants Based on the Normal-ized Difference Vegetation Index (NDVI) Value in Image of Unmanned Aircraft Case Study of Me-rauke-Papua Selatan. Engineering and Technology Journal 8(2): 1986-1991.

64. Asrar G, Fuchs M, Kanemasu ET, Hatfield JL (1984) Estimating absorbed photosynthetic ra-diation and leaf area index from spectral reflectance in wheat. Agron Journal 76(2): 300.

65. Rehman TH, Lundy ME, Linquist BA (2022) Comparative Sensitivity of Vegetation Indices Measured via Proximal and Aerial Sensors for Assessing N Status and Predicting Grain Yield in Rice Cropping Systems. Remote Sensing 14(12): 2770.

66. Feng A, Zhou J, Vories ED, Sudduth KA, Zhang M (2020) Yield estimation in cotton using UAV-based multi-sensor imagery. Biosystems Engineering 193: 101-114.64.

67. Zhou X, Zheng HB, Xu XQ, He JY, Ge XK, et al. (2017) Predicting grain yield in rice using multi-temporal vegetation indices from UAV-based multi-spectral and digital imagery. ISPRS Journal of Photogrammetry and Remote Sensing 130: 2

68. Noureldin NA, Aboelghar MA, Saudy HS, Ali AM (2013) Rice yield forecasting models using satellite imagery in Egypt. The Egyptian Journal of Remote Sensing and Space Science, 16(1): 125-131.

69. Huang Y, Lan Y, Qi H, Wu W (2014) Comparison of vegetation indices for monitoring rice growth. Remote Sensing Applications: Society and Environment 2: 48-60.

70. Xie Q, Yang L, Wang J (2020) Evaluation of vegetation indices for precision agriculture in rice fields. Journal of Applied Remote Sensing 14(3): 1-12.

71. Peng J, Xie Z, Zhang L, Li H (2018) Application of remote sensing technology for rice yield pre-diction in Southeast Asia. Agricultural Systems 161: 97-106.

72. Mikhail EM, James SB, Chris McGlone J. Introduction to modern photogrammetry. New York.

73. Dong J, Xiao X (2016) Evolution of regional to global paddy rice mapping: A review." ISPRS Journal of Photogrammetry and Remote Sensing, 119: 214-227.

74. Iizuka K, Fukumoto K, Tsuda S, Fukuda K, Hirose S (2018) Application of machine learning techniques for the estimation of crop yields in agricultural fields. Frontiers in Plant Science 9: 846.

75. Hangsheng L, Dan W, Jay B, Larry W (2005) Assessment of soil spatial variability at multiple scales. Ecological Modelling 182(3-4): 271-290.

76. Korie S, Clark SJ, Perry JN, Mugglestone MA, Bartlett PW, et al. (1998) Analyzing maps of dispersal around a single focus. Environmental and Ecological Statistics 5: 317-344.

77. Upchurch DR, Edmonds WJ (1991) Statistical procedures for specific objectives. Spatial varia-bilities of soils and landforms 28: 49-71.

78. Sampson Agyin-Birikorang, Ignatius Tindjina, Cisse Boubakary, Wilson Dogbe & Upendra Singh (2020) Resilient rice fertilization strategy for submergence In the Savanna agroecological zones of Northern Ghana, Journal of Plant Nutrition 43(7): 965-986.

79. Mazid Miah MA, Gaihre YK, Hunter G, Singh U, Hossain SA (2016) Fertilizer deep placement increases rice production: evidence from farmers' fields in southern Bangla-desh. Agronomy Journal 108(2): 805-812.

80. Khan R, Gurmani AR, Gurmani AH, Zia M (2007) Effect of phosphorus application on wheat and rice yields in the rice-wheat system. Sarhad J Agric 23(4).

DOI: 10.19080/ARTOAJ.2024.28.556425

How to cite this article: Andrew M, Vincent Kodjo A, Thomas J, Ama Twumasi D, Amisu M. Spatial Analysis of UAS-generated Data to Evaluate Nitrogen Fertilizer Placement Alternatives, Predict and Map End-of-Season Rice Yield. Agri Res& Tech: Open Access J. 2024; 28(5): 556425. DOI: 10.19080/ARTOAJ.2024.28.556425